THE JOURNAL OF PHYSICAL CHEMISTRY A

ARTICLE

pubs.acs.org/JPCA

Fast Nuclear Spin Conversion in Water Clusters and Ices: A Matrix Isolation Study

Russell Sliter, Melissa Gish, and Andrey F. Vilesov*

Department of Chemistry, University of Southern California, Los Angeles, California 90089, United States

ABSTRACT: Single water molecules have been isolated in solid Ar matrices at 4 K and studied by rovibrational spectroscopy using FTIR in the regions of the ν_1, ν_2, and ν_3 modes. Upon nuclear spin conversion at 4 K, essentially pure *para*-H_2O was prepared, followed by subsequent fast annealing generating ice particles. FTIR studies of the vapor above the condensed water upon annealing to $T \geq 250$ K indicate fast reconversion of nuclear spin to equilibrium conditions. Our results indicate that nuclear spin conversion is fast in water dimers and larger clusters, which preclude preparation of concentrated samples of *para*-H_2O, such as in ice or vapor.

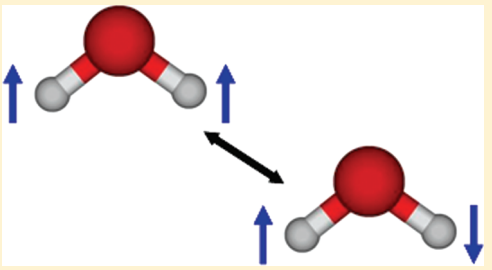

1. INTRODUCTION

It is well-known that H_2 exists in two forms, ortho and para, in which the total nuclear spin angular momentum is $I = 1$ and 0, respectively. Pure *para*-hydrogen, *p*-H_2, is usually obtained via cryogenic conversion of liquid hydrogen on para-magnetic salts.[1,2] Previous studies demonstrated that gaseous *p*-H_2 is remarkably stable at room temperature and can be stored for days with negligible back conversion.[3] A number of other molecules such as H_2O, NH_3, CH_2O, and CH_3F having equivalent hydrogen atoms are also known to have ortho and para nuclear spin isomers.[4]

The possibility of separating nuclear spin isomers in water molecules has attracted considerable attention[5−8] because of the fundamental atmospheric and biological significance of water. Measurements of the temperature of comets from the abundance ratio of the ortho and para isomers, OPR, have been proposed to determine the temperature of the primordial solar system.[9] Conversely, some recent works have questioned the enhancement of *para*-H_2O because of its negligible vapor pressure at 30 K and the extent to which the temperature of the water vapor corresponds to the temperature of the comet ice.[10] At equilibrium and temperatures larger than 50 K, the OPR of H_2O is very close to the statistical weight of 3:1. Therefore, practical spin conversion requires interaction of the water molecules with a low temperature bath of ≤10 K. However, the rotation of water molecules is quenched in ices such that the energy difference between the nuclear spin isomers in ice is presumed to be negligibly small. Thus, single water molecules have been isolated in cryogenic rare gas matrices,[11−19] where they continue rotating and demonstrate slow nuclear spin conversion at $T \leq 4$ K. Nevertheless, controversy remains if *para*-H_2O molecules are stable in ice, liquid, or gas. Previous works reported on the short lifetime of *p*-H_2O molecules in Ar matrices at higher temperatures.[15] Very recently, however, enrichment of *ortho*- and *para*-water via gas-phase chromatography has been reported with surprisingly long conversion times in liquid of ∼30 min.[20]

In this work, we studied the feasibility of the formation of *p*-H_2O ices. We began with the nuclear spin conversion of very diluted samples of water in Ar matrices that have been spin converted at $T = 4$ K in an enclosed cryogenic optical cell. The ice particles are formed from *p*-H_2O molecules upon fast increase in the temperature and removal of the Ar constituency from the cell. Finally, infrared spectra of the gas in the cell have been obtained at $T = 260-280$ K. The acquired spectra are identical to those of unconverted water, showing that the lifetime of *p*-H_2O in ice is less than ∼30 min. In addition, our results indicate that spin conversion already takes place in water dimers.

2. EXPERIMENTAL TECHNIQUE

The general technique of matrix deposition has been previously described.[18] Our cryogenic system is based on a Janis SHI-4 optical cryostat equipped with a Sumitomo RDK-408D closed-cycle refrigerator. The schematic of the copper cell is shown in Figure 1. The cell is directly attached to the second stage of the refrigerator. The gas is introduced through a stainless steel adaptor using copper tubing. The copper tubing is resistively heated to prevent freezing of the water mixture. The temperature of the cell was measured by silicone diodes and controlled by resistive heating.

Ar (Gilmore, 99.9999% purity)) was used without purification. Water was filtered (Milli-Q) and degassed carefully. H_2O/Ar mixtures ≤1:100 were prepared by standard manometric procedures. Because of adsorption of water onto the stainless steel walls of the gas handling system, the uncertainty in water content is estimated at 50%. The solid sample was prepared by depositing the gas mixture onto the CaF_2 window at a nominal

Special Issue: A: David W. Pratt Festschrift

Received: February 2, 2011
Revised: May 20, 2011
Published: June 14, 2011

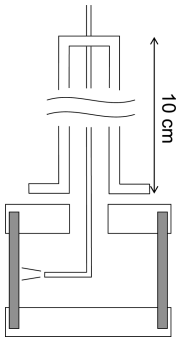

Figure 1. Schematic of cryogenic copper cell. The 3 cm long copper cell has an 18 mm diameter optical clearance enclosed by two 3 mm thick CaF_2 windows. The adjacent side of the cell provides a 9 mm clearance in which a stainless steel adapter with 1/16 in. thick copper tubing is attached for gas mixture introduction.

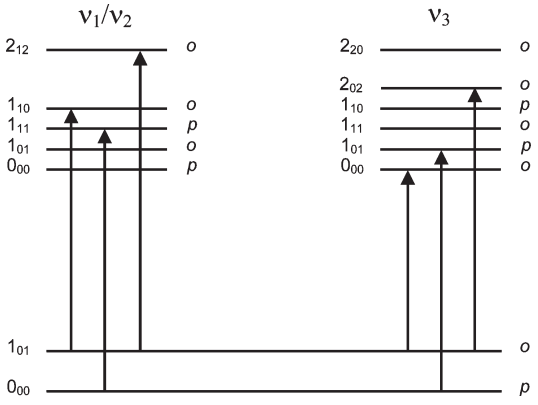

Figure 2. Energy level diagram of water molecules. Rotational level labels to the left of the lines represent $J_{K_aK_c}$ and correspond with the ortho and para labels on the right; *o* and *p*, respectively. Solid arrows indicate observed rovibrational transitions in ν_1, ν_2, and ν_3 bands at low temperature.

temperature of 4 K at a flow rate of ~10 mmol/h. The typical deposition time was between 40 and 70 min. Absorption spectroscopy was performed using a Nicolet Avatar 360 FTIR spectrometer in the 1000−4000 cm^{-1} region with a maximum resolution of 0.5 cm^{-1}. The quality of the sample during deposition was monitored by periodically recording scans.

3. RESULTS

Figure 2 shows a schematic of the relevant energy levels of water molecules in the ground and vibrationally excited states. Water is an asymmetric top molecule, and its rovibrational levels are labeled by $J_{K_aK_c}$, where J is the total rotational angular momentum quantum number and K_a and K_c are quantum numbers of the components of the total angular momentum on the principal axes *a* and *c*, respectively. These levels are assigned in the ground vibrational state as well as in ν_1 and ν_2 vibrationally excited states to either para or ortho species for even or odd $K_a + K_c$, respectively.[21] The notations are inverted in the antisymmetric vibrational ν_3 state. Because the total wave function of water molecules must be antisymmetric with respect to exchange of H atoms, it follows that the ground state of water molecules, 0_{00}, has a total nuclear spin $I = 0$, whereas the first

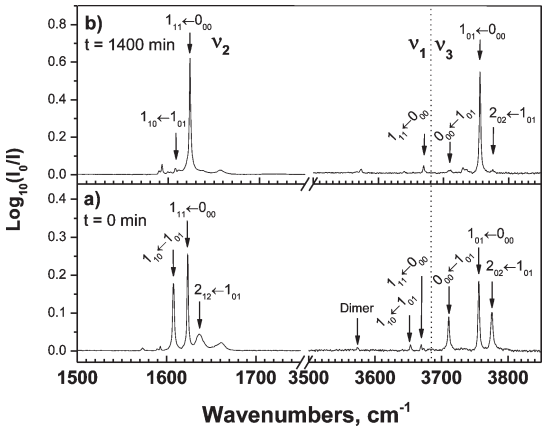

Figure 3. IR absorption spectra of the ν_1, ν_2, and ν_3 regions of H_2O of a 1:2000 H_2O/Ar sample. Panels (a) and (b) refer to spectra obtained after completing ~70 min deposition at a nominal temperature of 4 K and after an additional 1400 min, respectively.

excited rotational state, 1_{01} (E = 23.8 cm^{-1}),[22] has $I = 1$, which belongs to para- and ortho- nuclear spin isomers, respectively.

Figure 3a shows IR absorption spectra in the region of the ν_3, ν_2, and ν_1 bands of H_2O as obtained immediately after a deposition of 70 min at 4 K was completed. No annealing has been used to avoid cluster formation. Spectrum (a) corresponds to transitions from the lowest rotational levels of the *p*-H_2O and *o*-H_2O molecules, 0_{00} and 1_{01}, respectively, in agreement with previous observations.[18,19] The $0_{00} \leftarrow 1_{01}$, $1_{01} \leftarrow 0_{00}$, and $2_{02} \leftarrow 1_{01}$ lines of the ν_3 band of single H_2O molecules are assigned in the spectrum accordingly. The weak features at 3669.6 and 3653.3 cm^{-1} have been assigned to $1_{11} \leftarrow 0_{00}$ and $1_{10} \leftarrow 1_{01}$ lines of the ν_1 band, respectively. It is seen that the band due to water dimers at 3574 cm^{-1} is very weak, indicating that single water molecules are indeed isolated in the Ar matrix. Some weak features around 3730 cm^{-1} can be assigned to the ν_3 band of H_2O-N_2 complexes.[23−25]

Figure 3b was obtained after 1400 min time upon the completion of a ~ 70 min deposition, during which the matrix was kept at 4 K. It is seen that the same lines as those in Figure 3a are observed but with different intensities. Much weaker intensity of the lines from the 1_{01} levels and simultaneous increase in the intensity of the lines from 0_{00} levels indicates spin conversion. The total intensity of the lines from the ν_3 band in spectrum (a) before the conversion was found to be the same as that upon conversion within 20% accuracy. It should be noted that the OPR in spectrum (a) was found to be ~2 and not 3 as in the deposited water gas. This indicates that some conversion already proceeds during the deposition process. The spectra have been measured at intermediate conversion times. From the time dependence of the spectra, a conversion time of $\tau = 650 \pm 50$ min was obtained, which is comparable to what was previously observed in solid argon at 4 K.[12] From the intensity of the lines in trace (b), we have estimated the spin temperature of the water molecules to be ~6 K. This is somewhat higher than the measured temperature of the cell of 4 K due to the likely higher temperature of the optical window.

Spectra in the ν_2 region of H_2O are shown in the low-frequency range of Figure 3 and are in agreement with the findings from the other bands. Assigned transitions originate from the 1_{01} and 0_{00} levels of the ground state, as previously noted.[18,19] Some weak

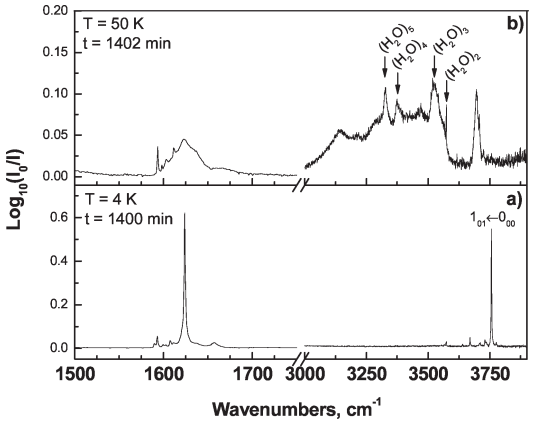

Figure 4. IR absorption spectra of the ν_1, ν_2 and ν_3 regions of H_2O in a 1:2000 H_2O/Ar sample at (a) 4 and (b) 50 K. Timeline refers to spectra obtained after completing ~70 min deposition of mixture.

features are also seen at 1593 and 1611 to 1612 cm^{-1} and are likely due to water dimers and H_2O-N_2 complexes, whereas features around 1600 and 1602 cm^{-1} originate solely from H_2O-N_2 complexes.[19,23,25,26]

Previously, an additional weak band at 1589.1 cm^{-1} was assigned to nonrotating monomers.[19,27] However, this frequency coincides with a known band of H_2O-CO_2 complexes.[17] Overall, we did not detect any additional bands that could be assigned to nonrotating water molecules in the ν_1 and ν_3 ranges of the spectra. Finally, a relatively intense and broad structure (10 cm^{-1}) at ~1660 cm^{-1} was assigned to rotation-translation satellites of the $1_{11} \leftarrow 0_{00}$ line.[18]

Figure 4 shows the evolution of the absorption spectrum upon fast temperature increase in the matrix. Figure 4a is equivalent to the single molecule spectra of Figure 3b, that is, at T = 4 K after conversion. Figure 4b shows a spectrum obtained upon heating the sample to T = 50 K within about 2 min. Spectrum (b) shows a broad, strong absorption in the range of 3000−3600 cm^{-1} and a narrower band close to 3700 cm^{-1}. These bands arise from the hydrogen bond bridge and free OH vibrations, respectively, in water clusters.[19,28,29] By analogy to the spectra of water clusters in He droplets,[14,30] bands at 3573.6, 3530, 3370, and 3320 cm^{-1} can be assigned to dimers, trimers, tetramers, and pentamers, respectively. Similar absorptions have also been previously observed in solid Ar.[23] The unresolved broad absorption in the range of 3000−3600 cm^{-1} must be due to larger water clusters.

The total integral intensity of spectrum (b) is a factor of ~10 larger than that in trace (a), which reflects a large increase in the infrared intensity upon formation of hydrogen bonds in clusters.[31] The factor of 10 is in qualitative agreement with the increase in the total infrared intensity in ice in the range of 3100−3800 cm^{-1} of ~20 as compared with that in the ν_3 mode of free water molecules.[31] The lower factor in this work is likely due to the fact that in clusters there remains a large number of dangling OH bonds, as indicated by the intense band around 3700 cm^{-1}.

Similar changes in the spectrum occur upon heating in the ν_2 spectral range. Upon increase in temperature, the lines of single molecules disappear. Simultaneously, a broad cluster feature in the range of 1600−1700 cm^{-1} appears as well as a narrow feature at 1593.4 cm^{-1}. The narrow band at 1593.4 cm^{-1} is not well understood but most likely represents bending modes of dangling

Table 1. Frequencies (cm^{-1}) and Assignments of Absorption Lines of Single H_2O Molecules in the ν_1, ν_2, and ν_3 Regions in Gas and in Solid Argon at 4 K

transition	spin isomer	gas[22]	in Ar, this work	in Ar, ref 18
ν_1 band				
$1_{10} \leftarrow 1_{01}$	ortho	3674.697	3653.3	3653.38
$1_{11} \leftarrow 0_{00}$	para	3693.293	3669.7	3669.85
ν_2 band				
$1_{10} \leftarrow 1_{01}$	ortho	1616.711	1607.7	1607.9
$1_{11} \leftarrow 0_{00}$	para	1634.967	1623.6	1623.8
$2_{12} \leftarrow 1_{01}$	ortho	1653.267	1636.7	1636.5
ν_3 band				
$0_{00} \leftarrow 1_{01}$	ortho	3732.134	3710.8	3711.2
$1_{01} \leftarrow 0_{00}$	para	3779.493	3756.1	3756.49
$2_{02} \leftarrow 1_{01}$	ortho	3801.419	3775.9	3776.30

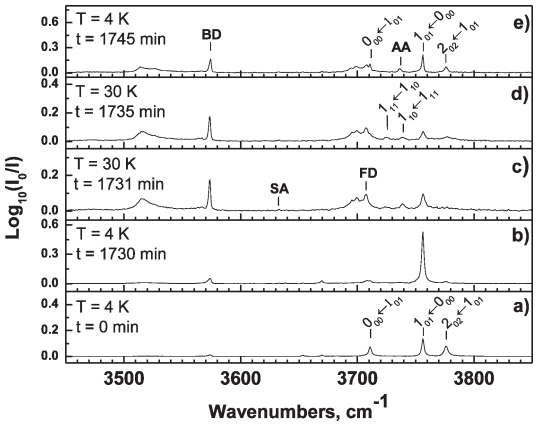

Figure 5. IR spectra in the ν_3/ν_1 region upon completion of ~40 min 1:1000 H_2O/Ar sample deposition at 4 K (a), ~1730 min conversion at 4 K (b), annealing to T = 30 K within 1 min (c), after continuous annealing for 5 min at 30 K (d), and after recooling the sample back to 4 K (e).

OH groups on clusters. The total integral intensity of spectrum (b) is only a factor of 1.7 larger as compared with that in trace (a). This is in agreement with a small change of the infrared intensity of the bending ν_2 band of water in ice.[31] A summary of the observed single-molecule peak positions in solid argon and assignments as well as comparison with gas phase[22] and previous work in argon[18] are provided in Table 1.

Previous works report fast decrease in the conversion time of the spin isomers of water molecules upon increase in temperature of the matrix.[12,18] Indeed, we have estimated the equilibration time of the nuclear spin isomers at 30 K to be ~5 min. Accurate measurements of the conversion time at higher matrix temperature are complicated by clustering and concomitant appearance of multiple cluster spectral features.

Fast spin interconversion impedes our ability to form water clusters entirely from p-H_2O molecules. Figure 5a−e demonstrate the stages of clustering observed upon completion of ~40 min 1:1000 H_2O/Ar sample deposition at 4 K (a), ~1730 min conversion at 4 K (b), annealing to 30 K for 1 min (c), continued annealing at T = 30 K for 5 min (d), and recooling back to 4 K (e). Upon immediate heating to 30 K, as observed in panel (c), the $1_{01} \leftarrow 0_{00}$ para transition at 3756 cm^{-1} is dominant despite

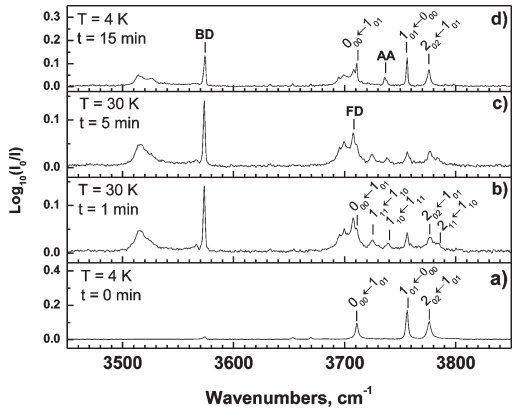

Figure 6. IR spectra of a 1:1000 H_2O/Ar sample in the ν_3/ν_1 region upon completion of ~40 min deposition at 4 K (a), annealing to T = 30 K within 1 min (b), after constant heating for 5 min at 30 K (c), and after recooling the sample back to 4 K (d).

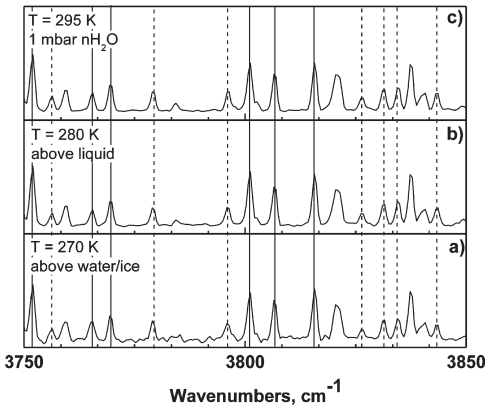

Figure 8. Magnified spectra of traces (b–d) from Figure 7 in the range of 3750–3850 cm^{-1}. Solid lines represent o-H_2O transitions, whereas dashed lines represent p-H_2O transitions.[22] Unlabeled lines represent overlaps of ortho and para transitions.

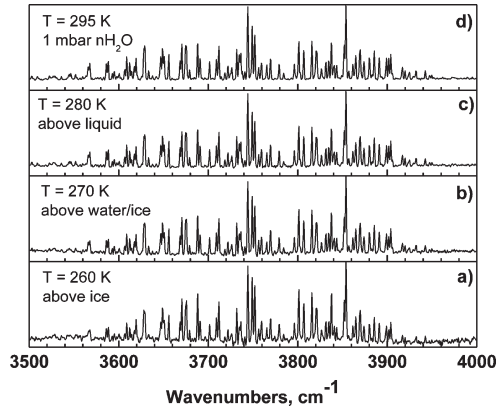

Figure 7. Normalized IR absorption spectra of ν_1/ν_3 region of H_2O at various temperatures after conversion to p-H_2O and subsequent fast annealing (a–c). (d) Comparable spectra of normal H_2O at 1 mbar and T = 295 K.

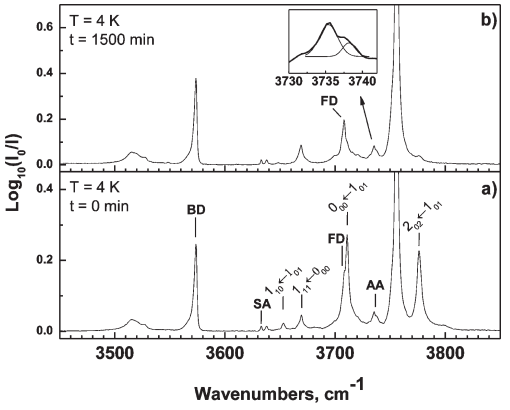

Figure 9. IR absorption spectra of ν_1/ν_3 region of 1:100 H_2O/Ar samples at T = 4 K after ~40 min completed deposition (a) and after 1500 min conversion (b). The panels are scaled to illustrate dimer features. The insert in panel b emphasizes the observed splitting of the AA band.

the onset of clustering. Therefore, we have concluded that small clusters are formed from predominantly p-H_2O molecules. In addition, we observed the growth of $1_{10} \leftarrow 1_{11}$ (para) and $1_{11} \leftarrow 1_{10}$ (ortho) transitions at 3738.8 and 3725.0 cm^{-1}, respectively. This trend persists upon continued annealing at T = 30 K for ~5 min (d). The spectrum of single water molecules obtained upon recooling the sample to T = 4 K indicates an OPR of ~1:1. Bound donor OH stretch (BD), free donor OH-stretch (FD), acceptor symmetric stretch (SA), and acceptor asymmetric stretch (AA) of water dimers are assigned in Figure 5c,e. The AA band is not clearly distinguishable at the higher temperature in panels (c–d) because of overlap with the $1_{10} \leftarrow 1_{11}$ line of water as well as the appearance of some broad background in the spectrum at T = 30 K.

Figure 6 shows spectra of a 1:1000 H_2O/Ar mixture after completing a ~40 min deposition at 4 K (a), similar to that in Figure 5, but upon immediate annealing to T = 30 K without spin conversion (b), continued annealing at 30 K for ~5 min (c), and after recooling down to T = 4 K (d). Despite the lack of time for sufficient conversion to occur as compared with spectra in Figure 5, similar features are observed.

We proceed with experiments designed to estimate the lifetime of *para*-water in ice. In these experiments, clusters have been formed upon rapid (5 min) heating of the converted samples from 4 to ~90 K. The matrix melts at ~90 K, and the Ar constituency was then removed from the cell by pumping. The cell containing ice particles was then heated within ~60 min up to T = 250 K to ensure sufficient vapor pressure of water for infrared analysis. Spectra were recorded at interval times throughout the heating process. Gas spectra of water could first be observed at $T \geq$ 250 K, as shown in Figure 7, for the ν_3/ν_1 region. Traces a–c represent spectra of water vapor above ice, ice/liquid, and liquid H_2O at T = 260, 270, and 280 K, respectively. A spectrum of unconverted H_2O at room temperature is provided in trace (d) in Figure 7 for convenience. All spectra were normalized for comparison. As observed, transitions originating from both ortho and para levels are present, where intensities are equal within experimental uncertainty to those obtained from an ordinary water sample. Figure 8 shows a magnified part of the spectra that contains identification of the lines originating from o- and p-water by solid and dashed lines, respectively. These observations indicate

Table 2. Band Origins and Rotational Constants (in wavenumbers) of Single Water Molecules in the ν_1, ν_2, and ν_3 Regions in Solid Argon at 4 K and in the Gas Phase

constants	gas[22]	in Ar, this work	in Ar, ref 18
		ν_1 band	
ν_0 (sym)[a]	3657.049	3638.4	3638.5
C	9.105	8.2	8.25
		ν_2 band	
ν_0 (sym)[a]	1594.752	1589.0	1589
C	9.134	8.0	8.11
		ν_3 band	
ν_0 (asym)	3755.950	3733.5	3733.5
$(B + C)/2$	11.77	11.3	11.5

[a] For calculation of ν_1/ν_2 band origins, positions of the $1_{11} \leftarrow 0_{00}$ lines and C constant from current work as well as A from ref 18 were used.

complete back-conversion of the p-H_2O sample during the course of the experiments.

Spectra of samples obtained upon deposition of mixtures having larger content of H_2O/Ar have also been studied. Figure 9 shows spectra of a 1:100 H_2O/Ar mixture after completing ~40 min deposition at 4 K (a) and after an additional ~1500 min at 4 K (b). The bands at 3573.6 cm^{-1} (1), 3633.0 cm^{-1} (0.02), 3708.1 cm^{-1} (0.45), and 3735.4 cm^{-1} (0.25) are assigned to (BD), (SA), (FD), and (AA), respectively. The relative intensities of the bands are given in parentheses. The band positions are in good agreement with previous Ar matrix studies.[17,19,23,25] Our recent He droplet study[32] gives the positions of the BD, SA, and FD bands to be 3597.4, 3654.2, and 3729.5 cm^{-1}, respectively, that is, having ~22 cm^{-1} blue shift with respect to corresponding frequencies in Ar matrix. The relative intensities of the dimer bands are in good agreement with those obtained in our He droplet study.[32] A weak feature at 3638 cm^{-1} corresponds to the H_2O-N_2 complex based on previous studies[23] and disappears upon stringent purging of the system. Close examination of the AA band in the inset in Figure 9b shows two closely spaced components having frequencies of 3735.4 and 3737.5 cm^{-1} and full widths of ~3 cm^{-1} each, as also previously observed in Ar matrix.[18,25]

4. DISCUSSION

The frequencies of the rovibrational lines of the ν_1, ν_2 and ν_3 bands from Table 1 were fitted to known expressions for the b- and a-type transitions of an asymmetric top, respectively, by employing effective rotational constants to account for the matrix environment.[33] Here we assume the same values of the rotational constants in the vibrationally excited state as in the ground state. Rotational constants and band origins obtained in this work are compared with the corresponding values in the gas phase[22] as well as in Ar matrix[18] in Table 2. Our results are very similar to the ones of ref 18. Because of the limited number of lines, the A rotational constant could not be obtained. All constants are ~10% smaller than those in the gas phase, which is consistent with the effects of a hindered rotation in the argon matrix.

Details of spin conversion of molecules inside matrices remain poorly understood. In the gas phase, spin conversion is believed to occur by the intramolecular mixing of ortho and para states of the molecule during collisions and has been discussed for several molecules such as CH_3F,[34] CH_4,[35] CCH_4,[36] and H_2O.[35] For water in the gas phase, for example, the nearest ortho and para states capable of coupling in the ground vibrational state are para $18_{15,3}$ and ortho $17_{10,7}$, which have energies of ~6869 cm^{-1}.[37] and are thus inaccessible in a cryomatrix. Of course, resonances between the ortho and para levels may occur at lower energy in matrices where rotational constants are different. Larger width of the rotational energy levels in the matrix will also facilitate the conversion. In addition, interaction with the matrix breaks the symmetry of the rotational wave function, allowing for spin-rotation coupling. As suggested by the increasing efficiency with temperature, conversion mostly likely involves interaction with phonons of the matrix.[38,39]

In the gas phase as well as in single water molecules isolated in a matrix, the relative stability of the spin isomers stems from the fact that ortho and para states belong to different rotational states having an energy difference of ~24 cm^{-1}; see Figure 1. However, in ice, intermolecular hydrogen bonding quenches molecular rotation, in which splitting between ortho and para states is estimated on the order of 10^{-2} Hz.[10] As a result, spin−spin interactions become important and mediate nuclear spin relaxation. Model calculations indicate nuclear spin relaxation in water dimers[10] within ~100 μs.

Figures 7 and 8 illustrated that upon annealing to T = 260−280 K, the spectra of previously converted H_2O are identical to within error limits of that of normal, unconverted H_2O. This observation indicates that the back-conversion of *para*-H_2O to thermal equilibrium occurs in <60 min, as limited by the time required to heat the cell to 260 K. In comparison, a recent study reported on the gas-chromatographic preparation and storage of *para*-ice and *para*-water samples over a time period of a few months and ~30 min time, respectively, without noticeable back conversion.[20] Other works have reported spin selectivity of H_2O by its interaction with porous surfaces of inorganic and organic materials[40,41] as well as in biological solutions.[42,43] However more recent experiments by Chapovsky et. al[44] failed to reproduce previous results.

Present work suggests that spin conversion of water clusters is fast in Ar matrices. Unfortunately, features due to different o-H_2O and p-H_2O compositions in larger clusters remain unresolved. However, some information can be gained from the AA band of dimers. The water dimer is a nearly symmetric prolate top with gas-phase rotational constants of about A = 7.6 cm^{-1} and $(B + C)/2$ = 0.205 cm^{-1}.[45] Hindered internal rotation of the acceptor molecule, commonly referred to as acceptor switching, results in the splitting of the dimer's energy levels into A_1^+ and A_2^- components of ~7 cm^{-1}.[46] As observed in helium droplets, the AA bands originating from the A_1^+ and A_2^- levels have two bands of comparable intensity separated by ~7.5 cm^{-1} due to dimers having para−para/ortho−para and ortho−ortho composition, respectively.[32] Therefore, nuclear spins in water dimers remain unrelaxed during the time-of-flight of ~3 ms, which is longer than 100 μs, as obtained in the aforementioned model calculations.[10]

On the basis of the shift of the ν_3 band origin of single H_2O molecules in solid Ar with respect to that in He droplets[16,47] and the gas phase,[22] the sub-bands of AA molecules in solid Ar are expected to red shift by ~23 cm^{-1}. The observed feature around 3736 cm^{-1} is in accordance with predictions of the $K_a' = 1 \leftarrow K_a'' = 0$, A_1^+ para dimer transition. The $K_a' = 1 \leftarrow K_a'' = 0$ transition from the A_2^- state, which is expected around 3730 cm^{-1}, was not observed in the Ar matrix. The relative intensities of the free (FD) and bonded (BD) OH-stretch of the donor in H_2O dimers to the AA band around 3736 cm^{-1} in solid

Ar agree to within 20% of the total intensity of the AA band obtained in He droplets.[32] The good agreement of the intensity measurements in Ar and in He droplets indicates that the band around 3736 cm^{-1} accounts for the total intensity of the AA band. The relative intensity of the two components of the AA band at 3735.4 and 3737.5 cm^{-1} was found to be independent of annealing and conversion time; see Figures 5, 6, and 9. Therefore, it is unlikely these components stem from different nuclear spin isomers in water dimers. Thus, we tentatively assign the splitting of the AA band to interaction with the Ar matrix. The lack of the second component of the AA band due to ortho−ortho dimers indicates fast nuclear spin relaxation of the dimer in the Ar matrix on the scale of a few minutes. A very recent Ar matrix study[48] has ascribed the split AA band to transitions from the same acceptor switching ground state into two degenerate excited acceptor switching states split by a matrix-induced rotational barrier.

Infrared spectra of water molecules in cometary tails have indicated a low OPR on the order of about 2.5:1, which is consistent with a spin temperature of ∼30 K.[5−7] As a result, some suggest that the obtained OPR could be a measure of the temperature at which cometary ice is formed. According to this theory, the OPR in cometary ices is preserved over the time of 4.5 billion years, during which comets are mostly at 50 K or less, then heated briefly to temperatures higher than 180 K, at which point they sublimate. However, our spectra of water vapor (at T = 260 K) above ice, originally prepared from *para*-water molecules, show thermal OPR. Unfortunately, because of the low vapor pressure of water below T = 250 K and concomitant insufficient optical density, we are unable to study the molecules subliming at 180 K, such as in outer space. Nevertheless, our matrix isolation results of single water molecules show that at temperatures as low as 30 K spin conversion of single water molecules and dimers proceeds within minutes. As a result, long time stability of *para*-water molecules in ices at higher temperatures seems unlikely, and the conclusion that cometary formation temperatures can be probed using the OPR ratios is in doubt.

5. CONCLUSIONS

In this work, we have studied the rovibrational spectra of single water molecules isolated in solid Ar matrices in the range of ν_1, ν_2, and ν_3 bands using FTIR spectroscopy. Using nuclear spin conversion at T = 4 K, we have prepared highly enriched samples of *para*-H_2O. Upon fast annealing, we generated ice particles and studied their corresponding vapor from T = 260 to 280 K. In comparison with normal H_2O, FTIR studies of the vapor indicate reconversion of nuclear spins to equilibrium conditions. Subsequent experiments of water dimers in solid Ar have been performed in which all four OH-stretching bands (AA, FD, SA, and BD) were observed. The observation of a single AA feature indicates fast nuclear spin relaxation into the *para*-$(H_2O)_2$ configuration. As a result, the preparation of concentrated samples of *para*-H_2O, such as in ice or vapor, is unfeasible.

■ ACKNOWLEDGMENT

We are grateful to Melody Sun and for her help with some of the experiments described in this Article. We are also grateful to Boris Sartakov, Murthy Gudipaty, and David Jewitt for stimulating discussions. This material is based on work supported by the NSF under grant CHE 0809093.

■ REFERENCES

(1) Momose, T.; Shida, T. *Bull. Chem. Soc. Jpn.* **1998**, *71*, 1.
(2) Kuyanov, K. E.; Momose, T.; Vilesov, A. F. *Appl. Opt.* **2004**, *43*, 6023.
(3) Farkas, A. *Orthohydrogen, Parahydrogen, and Heavy Hydrogen*; Cambridge University Press: London, 1935.
(4) Hertzberg, G. *Molecular Spectra and Molecular Structure, II Infrared and Raman Spectra of Polyatomic Molecules*; Van Nostrand Reinhold Company: New York, 1945.
(5) Mumma, M. J.; Weaver, H. A.; Larson, H. P. *Astron. Astrophys.* **1987**, *187*, 419.
(6) Dello Russo, N.; Bonev, B. P.; DiSanti, M. A.; Mumma, M. J.; Gibb, E. L.; Magee-Sauer, K.; Barber, R. J.; Tennyson, J. *Astrophys. J.* **2005**, *621*, 537.
(7) Kawakita, H.; Dello Russo, N.; Furusho, R.; Fuse, T.; Watanabe, J.; Boice, D. C.; Sadakane, K.; Arimoto, N.; Ohkubo, M.; Ohnishi, T. *Astrophys. J.* **2006**, *643*, 1337.
(8) Chapovsky, P. L.; Hermans, L. J. F. *Annu. Rev. Phys. Chem.* **1999**, *50*, 315.
(9) Crovisier, J. *Mol. Phys.* **2006**, *104*, 2737.
(10) Buntkowsky, G.; Limbach, H. H.; Walaszek, B.; Adamczyk, A.; Xu, Y.; Breitzke, H.; Schweitzer, A.; Gutmann, T.; Wachtler, M.; Frydel, J.; Elnmler, T.; Amadeu, N.; Tietze, D.; Chaudret, B. *Z. Phys. Chem.* **2008**, *222*, 1049.
(11) Redington, R. L.; Milligan, D. E. *J. Chem. Phys.* **1962**, *37*, 2162.
(12) Abouaf-Marguin, L.; Vasserot, A. M.; Pardanaud, C.; Michaut, X. *Chem. Phys. Lett.* **2007**, *447*, 232.
(13) Abouaf-Marguin, L.; Vasserot, A. M.; Pardanaud, C.; Michaut, X. *Chem. Phys. Lett.* **2009**, *480*, 82.
(14) Slipchenko, M. N.; Kuyanov, K. E.; Sartakov, B. G.; Vilesov, A. F. *J. Chem. Phys* **2006**, *124*, 241101.
(15) Hopkins, H. P.; Curl, R. F.; Pitzer, K. S. *J. Chem. Phys.* **1968**, *48*, 2959.
(16) Kuyanov, K. E.; Slipchenko, M. N.; Vilesov, A. F. *Chem. Phys. Lett.* **2006**, *427*, 5.
(17) Michaut, X.; Vasserot, A. M.; Abouaf-Marguin, L. *Low Temp. Phys.* **2003**, *29*, 852.
(18) Michaut, X.; Vasserot, A. M.; Abouaf-Marguin, L. *Vib. Spectrosc.* **2004**, *34*, 83.
(19) Perchard, J. P. *Chem. Phys.* **2001**, *273*, 217.
(20) Tikhonov, V. I.; Volkov, A. A. *Science* **2002**, *296*, 2363.
(21) Tennyson, J.; Zobov, N. F.; Williamson, R.; Polyansky, O. L.; Bernath, P. F. *J. Phys. Chem. Ref. Data* **2001**, *30*, 735.
(22) Rothman, L. S.; Gordon, I. E.; Barbe, A.; Benner, D. C.; Bernath, P. E.; Birk, M.; Boudon, V.; Brown, L. R.; Campargue, A.; Champion, J. P.; Chance, K.; Coudert, L. H.; Dana, V.; Devi, V. M.; Fally, S.; Flaud, J. M.; Gamache, R. R.; Goldman, A.; Jacquemart, D.; Kleiner, I.; Lacome, N.; Lafferty, W. J.; Mandin, J. Y.; Massie, S. T.; Mikhailenko, S. N.; Miller, C. E.; Moazzen-Ahmadi, N.; Naumenko, O. V.; Nikitin, A. V.; Orphal, J.; Perevalov, V. I.; Perrin, A.; Predoi-Cross, A.; Rinsland, C. P.; Rotger, M.; Simeckova, M.; Smith, M. A. H.; Sung, K.; Tashkun, S. A.; Tennyson, J.; Toth, R. A.; Vandaele, A. C.; Vander Auwera, J. *J. Quant. Spectrosc. Radiat. Transfer* **2009**, *110*, 533.
(23) Hirabayashi, S.; Ohno, K.; Abe, H.; Yamada, K. M. T. *J. Chem. Phys.* **2005**, 122.
(24) Kuma, S.; Slipchenko, M. N.; Kuyanov, K. E.; Momose, T.; Vilesov, A. F. *J. Phys. Chem. A* **2006**, *110*, 10046.
(25) Coussan, S.; Loutellier, A.; Perchard, J. P.; Racine, S.; Bouteiller, Y. *J. Mol. Struct.* **1998**, *471*, 37.
(26) Pardanaud, C.; Vasserot, A. M.; Michaut, X.; Abouaf-Marguin, L. *J. Mol. Struct.* **2008**, *873*, 181.
(27) Engdahl, A.; Nelander, B. *J. Mol. Struct.* **1989**, *193*, 101.
(28) Bentwood, R. M.; Barnes, A. J.; Orvillethomas, W. J. *J. Mol. Spectrosc.* **1980**, *84*, 391.
(29) Buck, U.; Huisken, F. *Chem. Rev.* **2000**, *100*, 3863.
(30) Burnham, C. J.; Xantheas, S. S.; Miller, M. A.; Applegate, B. E.; Miller, R. E. *J. Chem. Phys.* **2002**, *117*, 1109.

(31) Bertie, J. E.; Ahmed, M. K.; Eysel, H. H. *J. Phys. Chem.* **1989**, *93*, 2210.
(32) Kuyanov-Prozument, K.; Choi, M. Y.; Vilesov, A. F. *J. Chem. Phys.* **2010**, 132.
(33) Bernath, P. F. *Spectra of Atoms and Molecules*; Oxford University Press: New York, 1995.
(34) Chapovsky, P. L. *Zh. Eksp. Teor. Fiz.* **1990**, *97*, 1585.
(35) Curl, R. F.; Kasper, J. V. V.; Pitzer, K. S. *J. Chem. Phys.* **1967**, *46*, 3220.
(36) Chapovsky, P. L.; Ilisca, E. *Phys. Rev. A* **2001**, 6306.
(37) Miani, A.; Tennyson, J. *J. Chem. Phys.* **2004**, *120*, 2732.
(38) Miyamoto, Y.; Fushitani, M.; Ando, D.; Momose, T. *J. Chem. Phys.* **2008**, 128.
(39) Scott, P. L.; Jeffries, C. D. *Phys. Rev.* **1962**, *127*, 32.
(40) Potekhin, S. A.; Khusainova, R. S. *Biophys. Chem.* **2005**, *118*, 84.
(41) Tikhonov, V. I.; Makurenkov, A. M.; Artemov, V. G.; Porodinkov, O. E.; Volkov, A. A. *Phys. Wave Phenom.* **2007**, *15*, 106.
(42) Bunkin, A. F.; Pershin, S. M.; Nurmatov, A. A. *Laser Phys. Lett.* **2006**, *3*, 275.
(43) Bunkin, A. F.; Lebedenko, S. I.; Nurmatov, A. A.; Pershin, S. M. *Quantum Electron.* **2006**, *36*, 612.
(44) Veber, S. L.; Bagryanskaya, E. G.; Chapovsky, P. L. *J. Exp. Theor. Phys.* **2006**, *102*, 76.
(45) Keutsch, F. N.; Goldman, N.; Harker, H. A.; Leforestier, C.; Saykally, R. J. *Mol. Phys.* **2003**, *101*, 3477.
(46) Huang, Z. S.; Miller, R. E. *J. Chem. Phys.* **1989**, *91*, 6613.
(47) Lindsay, C. M.; Douberly, G. E.; Miller, R. E. *J. Mol. Struct.* **2006**, *786*, 96.
(48) Ceponkus, J.; Uvdal, P.; Nelander, B. *J. Chem. Phys.* **2010**, 133.